Energetic Protons and Electrons in the
Magnetotail of Jupiter

FIGURE CAPTIONS:

Fig. 1 Encounter trajectories for Voyager 1, 2, and Pioneer 10.

Fig. 2 Schematic drawing of the Voyager LET instrument. The detectors are enclosed in an aluminum housing with an average thickness of 0.025 inches.

Fig. 3 Look directions of the Voyager 1 LET's characteristic of the outbound pass projected into equatorial and meridinal planes. Positions shown were exact at 55 R_J.

Fig. 4 5 Proton and electron fluxes observed during the outbound passes of Voyager 1 and 2.

Fig. 6 Proton momentum spectra for 64 min. intervals observed during the outbound pass of Voyager 1. Spectra at 34.2, 59.0, 64.9, and 116.9 R_J where observed near neutral sheet crossings; the 42.4 R_J spectrum represents interplanetary particles observed 15° above the magnetic equator; the 146 R_J spectrum shows the particle population observed prior to the first magnetopause crossing.

Fig. 7 Result of least squares fit to 64 min. averages of the Voyager 1 LET A pulse height distributions. A differential spectrum of the form $j(E)=KE^{-1/2} \exp. -\sqrt{E/E_o}$ was fit to the data. The top panel shows the differential flux at 1 MeV and the lower panel gives the characteristic energy, E_o.

Fig. 8 Field aligned flow of protons with energies above 0.4 MeV away from Jupiter observed with Voyager 1 near 98 R_J. LET B is pointed nearly along the field line towards the planet and LET A perpendicular to it. The peak flux in LET B of 830 protons/cm^2sec ster is about 40 times the flux observed at the other neutral sheet crossings near 100 R_J.

Fig. 9 Proton momentum spectra averaged over 64 min. observed during the streaming event near 98 R_J. The spectrum of protons streaming along B is characteristic of particles trapped near the neutral sheet. The near 90° pitch angle particles (LET A) have a spectrum similar to that observed in the acceleration event near 59 R_J.

Fig. 10 Comparison of Voyager 2 neutral sheet crossings at various distances from Jupiter. LET A is indicated by X, LET C by □, and LET D by ● .

Fig. 11 Corrected longitude of the Voyager 2 neutral sheet crossings for the leading and lagging maxima.

FIG. 12 Corrected longitudes for the Voyager 1 and Pioneer neutral sheet crossings.

Fig. 13 Position of neutral sheet for I rigid disk and II hinged disk. Projections into meridional plane illustrates the case of no phase delay and projection into the curved plane illustrates the actual case with a delay (see test for definition of symbols).

Fig. 14 Illustrations of neutral sheet stream lines vs radius for different velocities in the active and inactive hemisphere. Notice rarification region at transition from inactive to active hemispheres and enhanced flux region at transition from inactive to active hemisphere.

Fig. 15 Voyager 1 observations of magnetotail and sheath electrons fluxes synchronized with the clock model.

Fig. 16 Voyager 2 observations of electron intensity ratios between 120 and 200 R_J showing frequent synchronization with clock model.

TABLE I

	Spacecraft Longitude from Subsolar Point				Distance at Magnetopause Crossing (R_J)
	At: 20 R_J	50 R_J	100 R_J	150R_J	
Voyager 2	177	-150	-140	-137	> 170
Voyager 1	-140	-123	-118	-115	158-165
Pioneer 10	-107	- 95	- 90	- 87	97-150

TABLE II

CRS DETECTORS USED DURING JUPITER ENCOUNTER

Detector	Shielding	Energy Range+ (MeV)	Factor (cm^2 ster)	Comments
Protons (LET)				
L1*	0.8 mg/cm^2 Aℓ	0.42 - 12	4.8	Also, Alphas above 0.32 MeV/n
L2*	8.1 mg/cm^2 Si	1.8 - 13	0.43	Through L1
counts twice as much as it would if all L_2 were $L_1 \cdot L_2$ $\overline{L_1}$ L_2	>140 mg/cm^2 Aℓ	>9	8.4	Protons through side comparable to those through front for E^{-2} spectrum
L1 L2 L4		1.8 - 8	0.43	ΔE - E analysis
L1 L2 L3 $\overline{L4}$		3 - 8	0.43	ΔE_1, ΔE_2 - E analysis
Electrons (HET)				
0.15 mm Si detector	0.9 mg/cm^2 Mylar		∿25	Responds primarily to 0.1-0.4 MeV electrons
Range 4 -10 mm Si	"	2.6 - 5.1	1.46	Coincidence rates with good background rejections, but accidental coincidence problems at high counting rates
10 - 16 mm Si	"	5.1 - 8	1.25	
16 - 22 mm Si	"	8 - 12	0.96	
Electrons (TET)				
D_1 (3 mm Si)*		>0.5 MeV	∿14	Usable at higher flux than HET rates
D_3 (3 mm Si)	∿1.2 cm Si equivalent	>5 MeV	∿14	" " " " " " "
Various Coincidence Combinations		2 to 50 MeV	3.1 to 0.66	

*Single Rates

+Small Difference Between Similar Detectors

TABLE III

OBSERVATIONS OF PROTONS STREAMING AWAY FROM JUPITER

DOY	DATE	TIME	DISTANCE	
VOYAGER 1				
70	3/11	500 to 700	98 R_J	Outward flow within 15° of magnetic field direction intensity ratio 0 to 90° pitch angles 40:1.*
72	3/13	1600 to 1830	133 R_J	Outward flow along B, intensity ratio 20:1.*
76	3/17	1100 to 1300	188 R_J	Outward flow from Jupiter in mangetosheath region, intensity ratio 2:1* (2-5 MeV electrons ratio 1.5).
VOYAGER 2				
203	7/22	800 to 1200	155 R_J	Outward flow along swept back field directions, intensity ratio 20:1 for detectors not well aligned with field. This event was also observed at low energies (Krimigis et al., 1980).
207	7/26	1200 to 1600	200 R_J	Outward flow but less extreme than the 7/22 event.

*Intensity ratio of >0.41 MeV protons between LET B and LET A.

TABLE IV

APPARENT VELOCITY INTO THE MAGNETOTAIL OF THE CHANGES IN THE POSITION OF THE NEUTRAL SHEET PRODUCED BY THE ROTATION OF THE TILTED MAGNETIC DIPOLE

RANGE	ACTIVE R_J/HR	INACTIVE R_J/HR	
20 - 65 R_J	---	46 $\pm$ 15	PIONEER 10
	20.4 $\pm$ 2.1	50 $\pm$ 21	10.4° NEUTRAL SHEET
	19.6 $\pm$ 1.9	56 $\pm$ 26	10.4 - 6.2°
70 - 140 R_J	46 $\pm$ 23	49 $\pm$ 12	10.4°
	57 $\pm$ 33	46 $\pm$ 15	10.4 - 6.2°

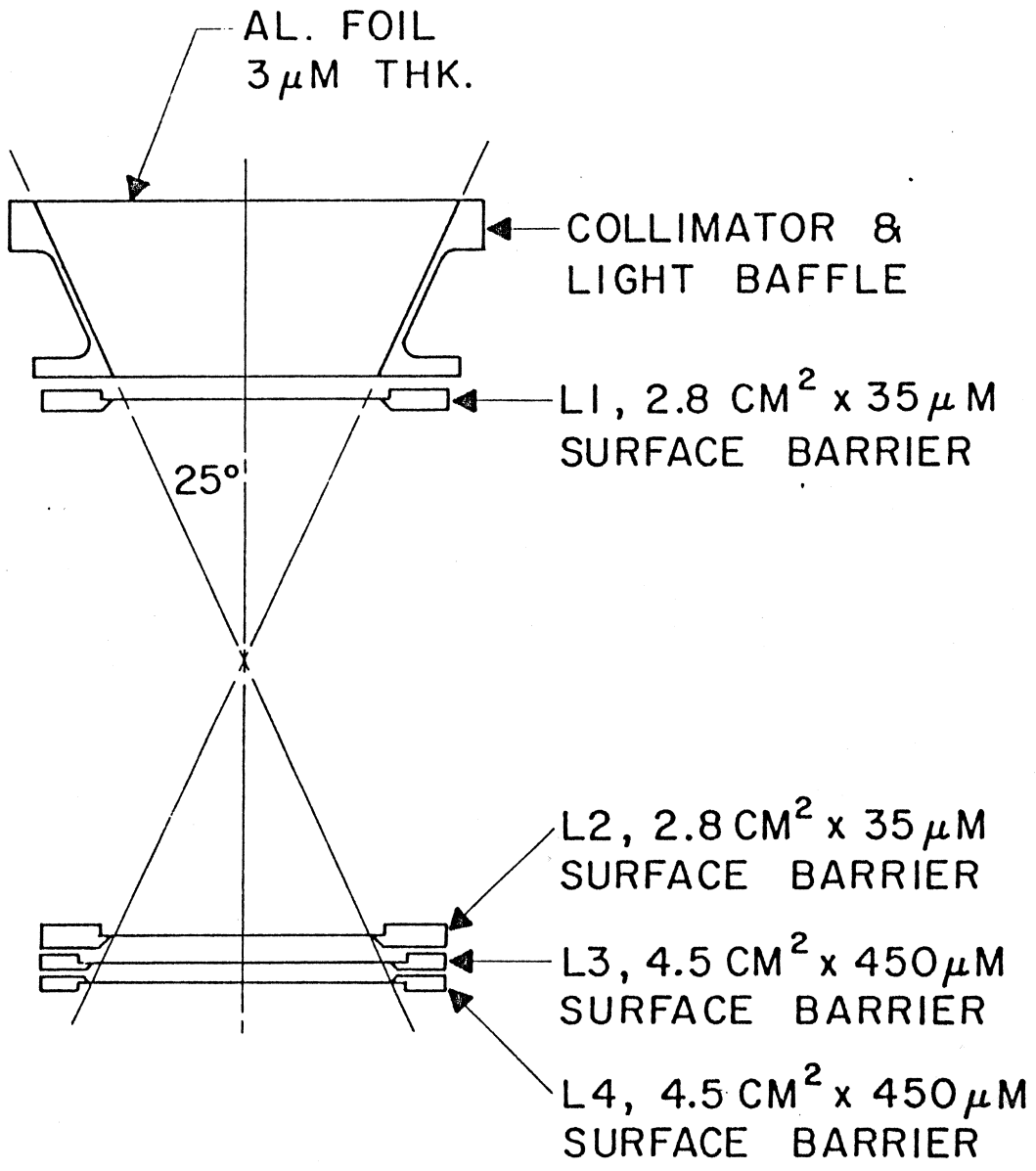

LOW ENERGY TELESCOPE (LET)

Fig. 2

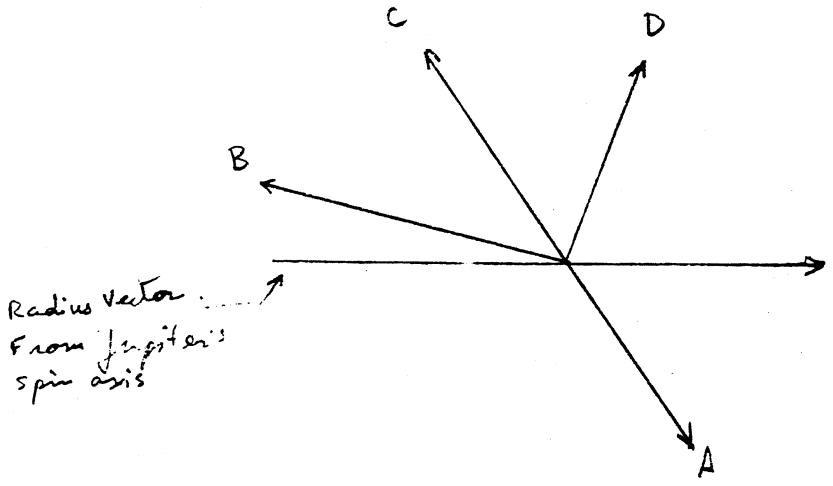

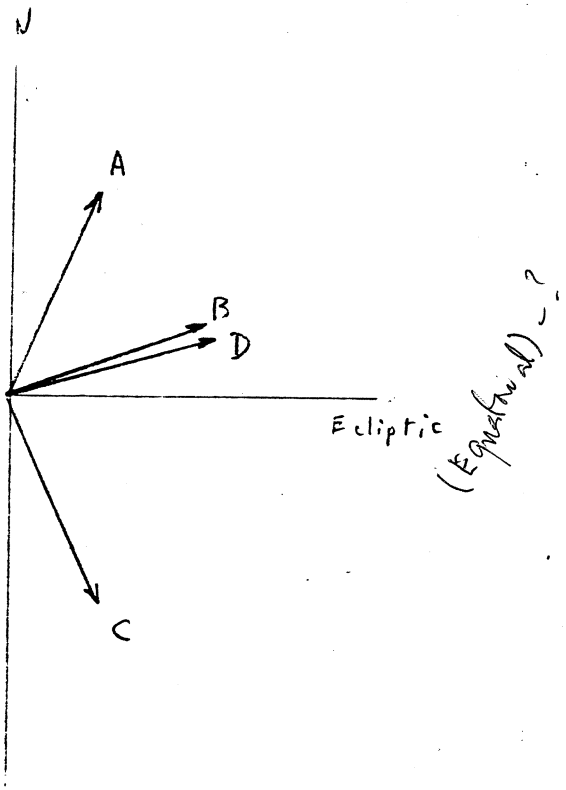

Outbound
Vectors went from direction (ϕ)
+15 on 3/6 to −10 on 3/15

Fig 3

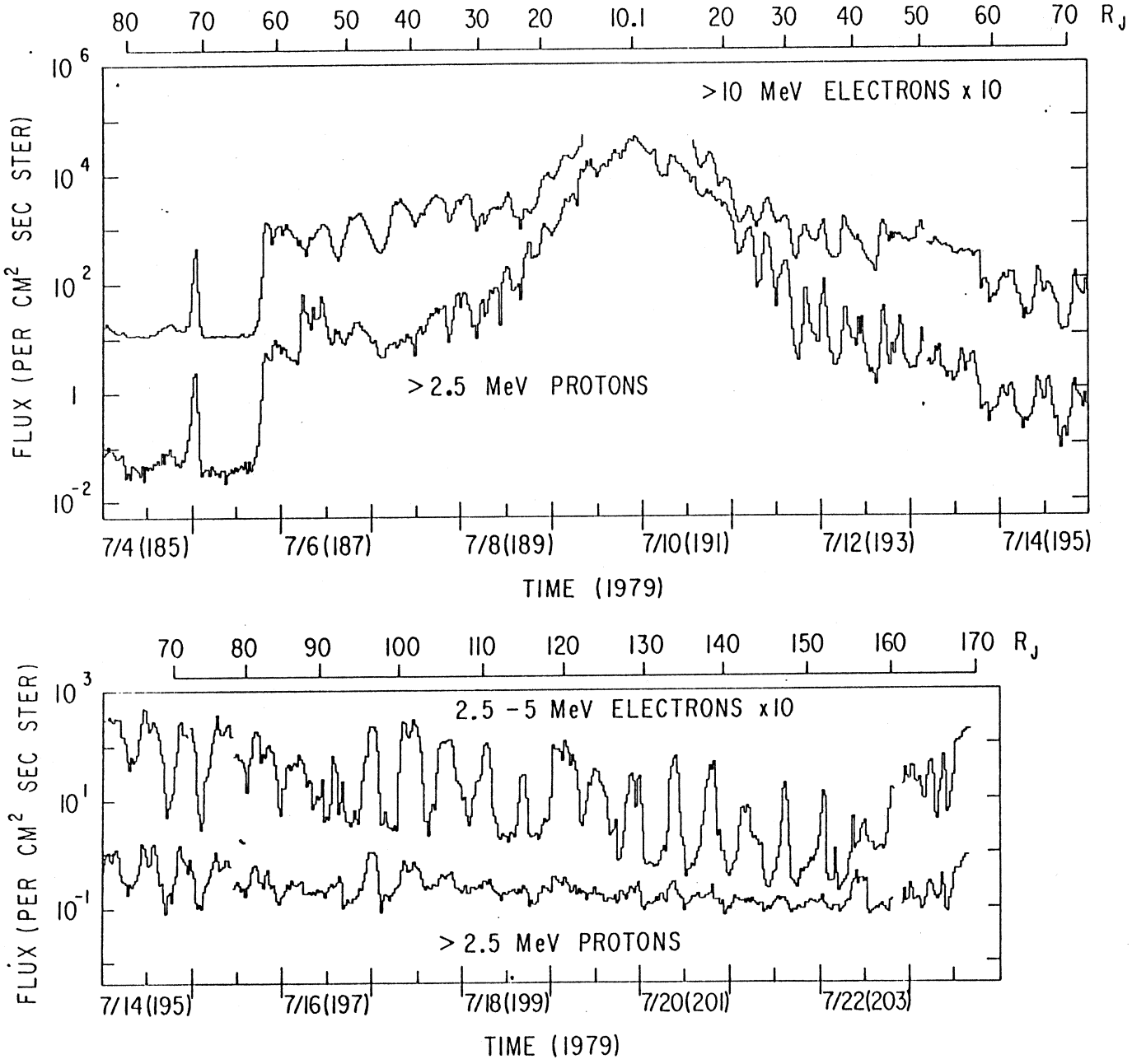

Fig 4 & 5 will be something like this for outbound pass & have not yet been made

higher latitudes
lack of
Gretation

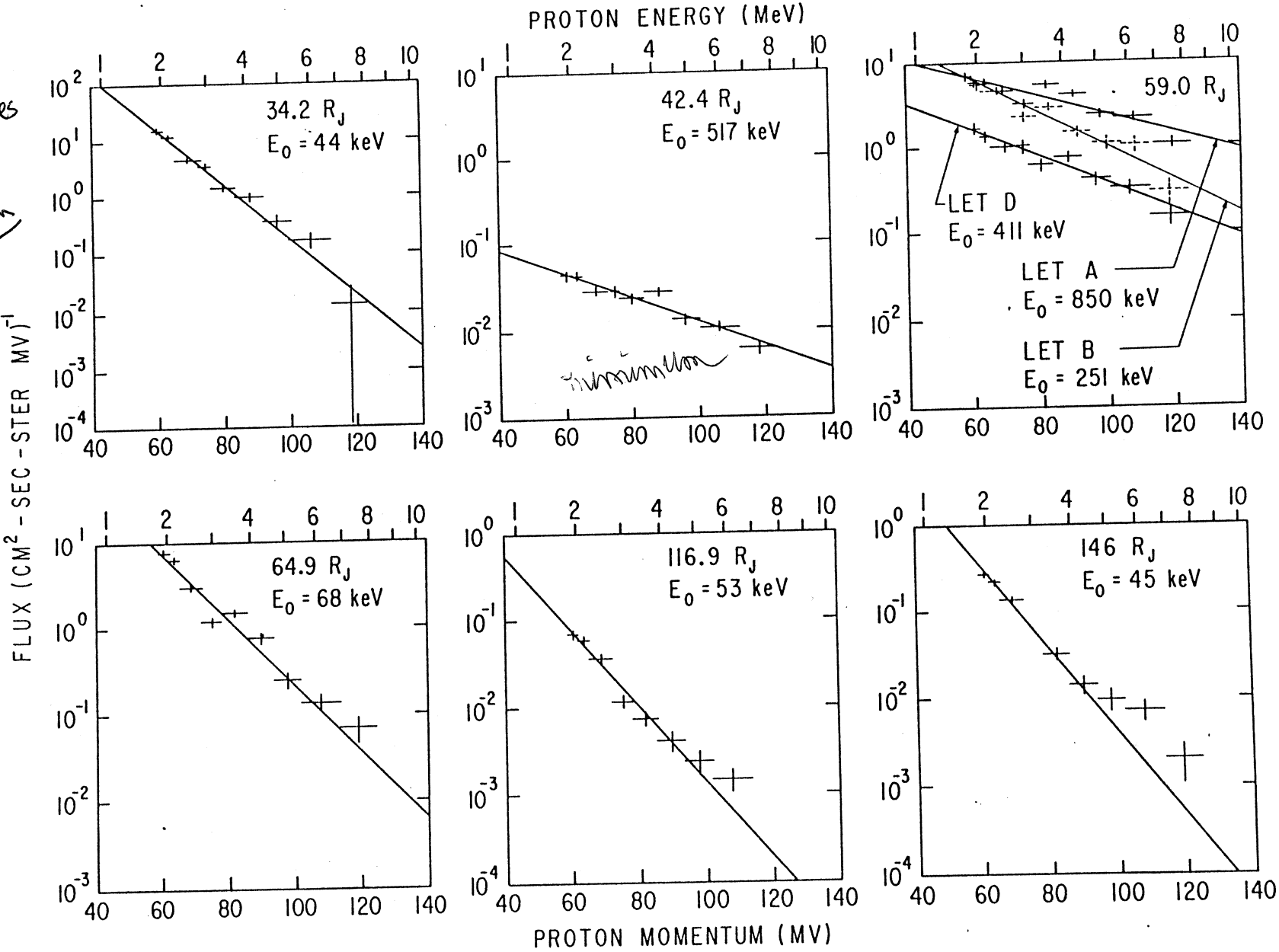

Fig 6

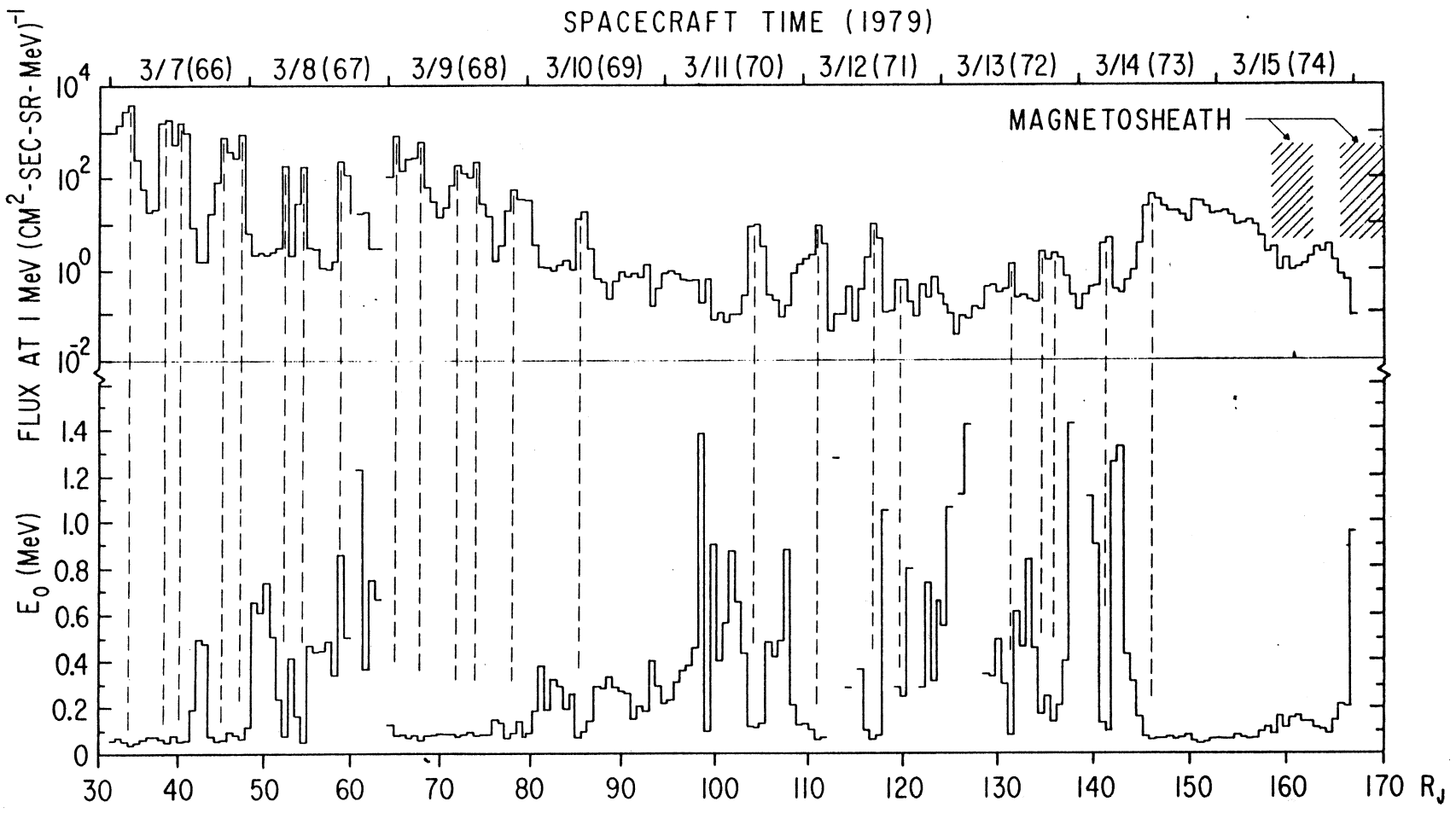
SPACECRAFT TIME (1979)
3/7(66)
3/8(67)
3/9(68)
3/10(69)
3/11(70)
3/12(71)
3/13(72)
3/14(73)
3/15(74)
MAGNETOSHEATH
FLUX AT 1 MeV (CM^2-SEC-SR-MeV)$^{-1}$
10^4
10^2
10^0
10^{-2}
E_0 (MeV)
1.4
1.2
1.0
0.8
0.6
0.4
0.2
0
30
40
50
60
70
80
90
100
110
120
130
140
150
160
170 R_J

Fig. 7

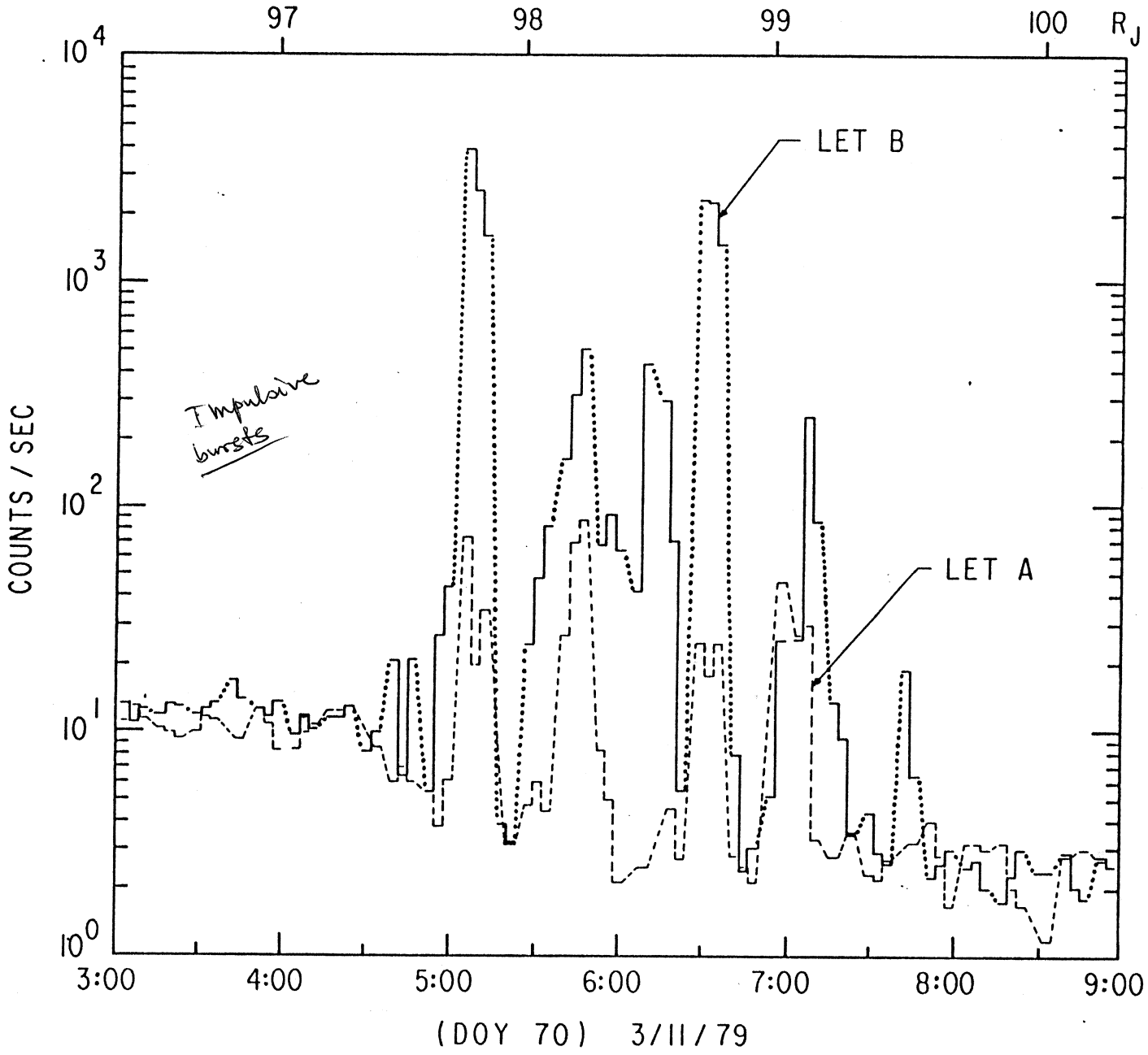
97
98
99
100
R_J
10^4
10^3
10^2
10^1
10^0
COUNTS / SEC
LET B
LET A
Impulsive bursts
3:00
4:00
5:00
6:00
7:00
8:00
9:00
(DOY 70) 3/11/79

Fig 8

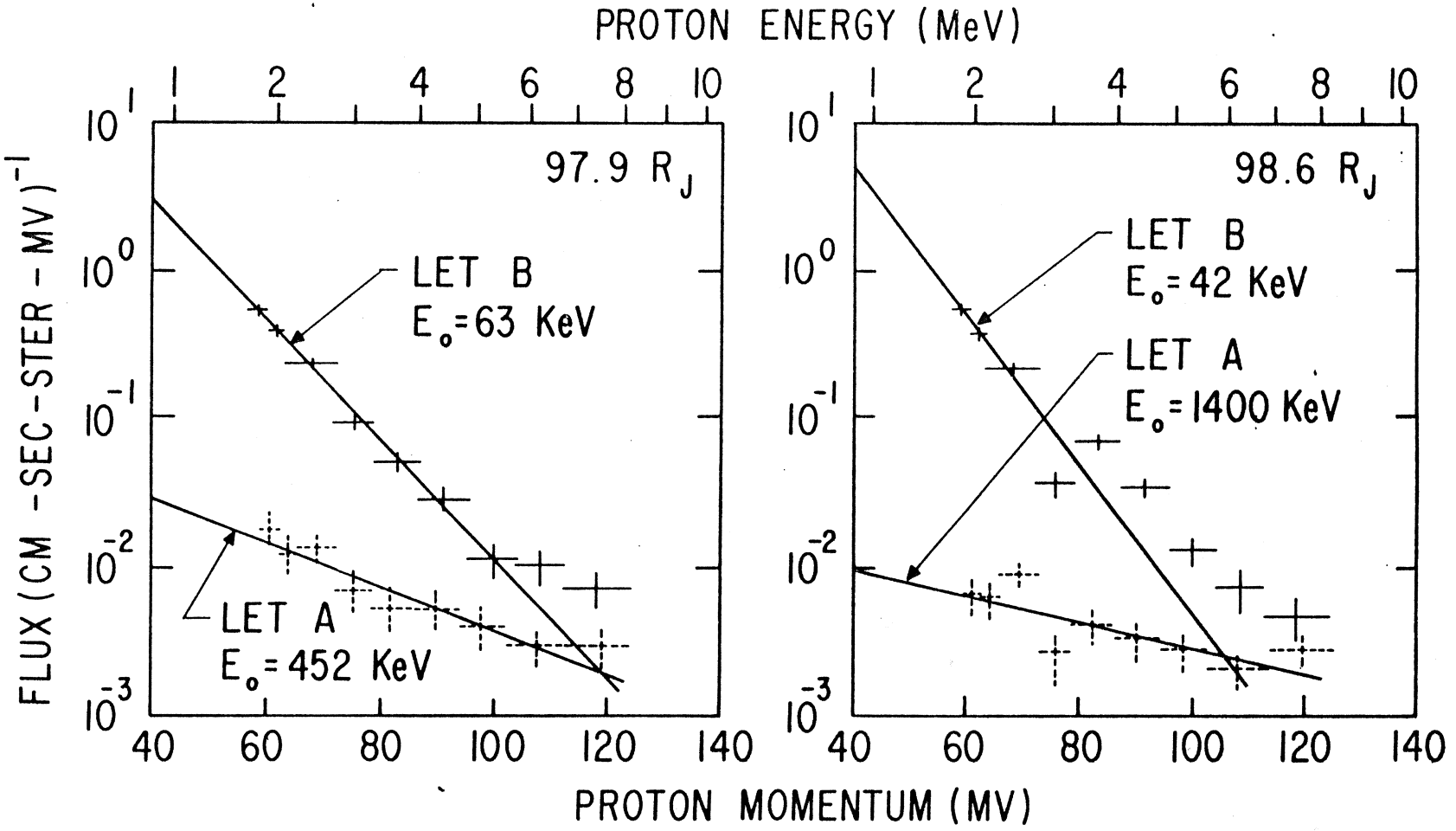
PROTON ENERGY (MeV)
1
2
4
6
8
10
10^{1}
10^{0}
10^{-1}
10^{-2}
10^{-3}
FLUX (CM -SEC-STER - MV)$^{-1}$
97.9 R_J
LET B
E_o=63 KeV
LET A
E_o=452 KeV
98.6 R_J
LET B
E_o=42 KeV
LET A
E_o=1400 KeV
40
60
80
100
120
140
PROTON MOMENTUM (MV)

Fig 9

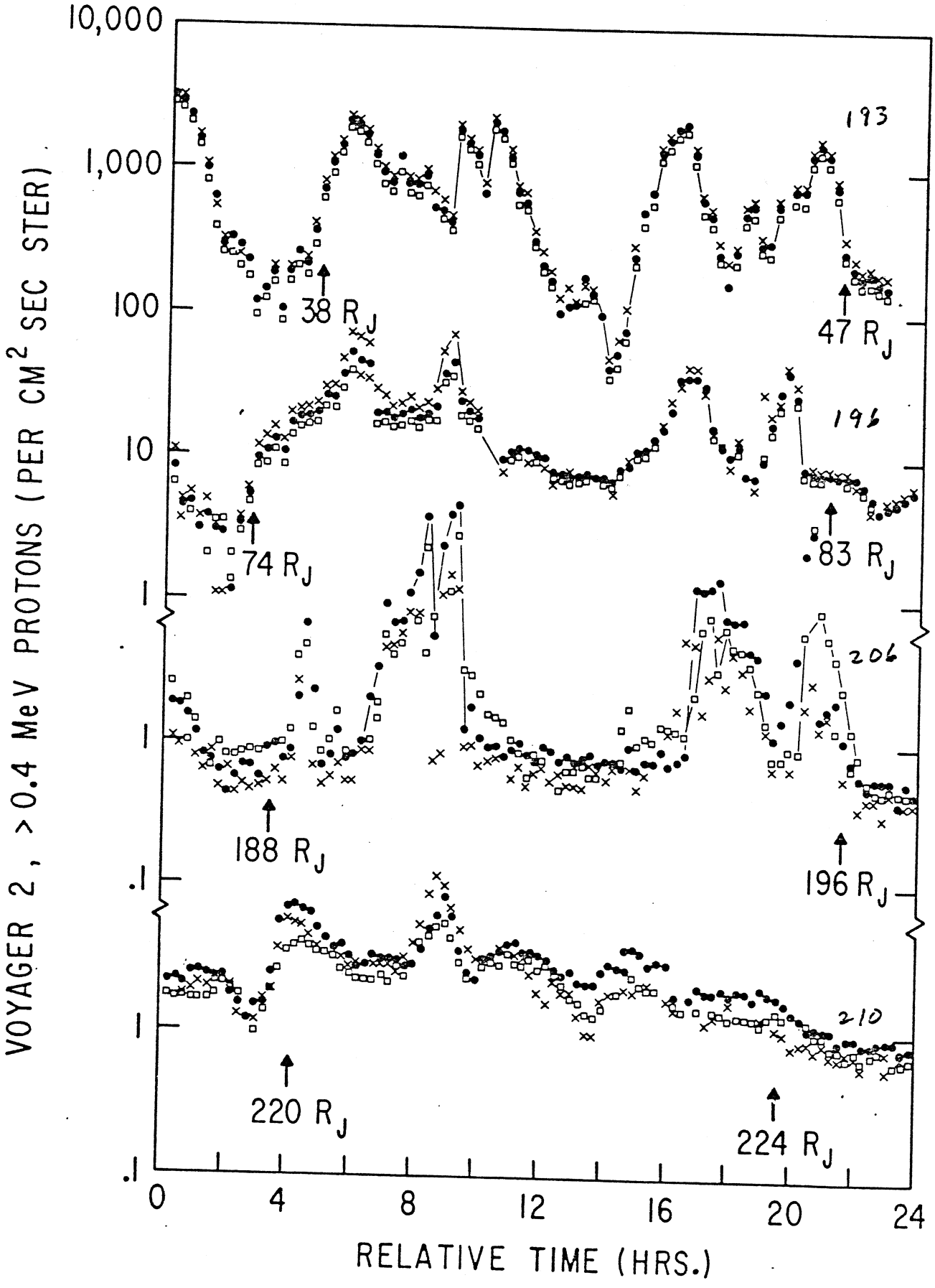
10,000
1,000
100
10
1
1
.1
1
.1
VOYAGER 2, >0.4 MeV PROTONS (PER CM² SEC STER)
193
38 R_J
47 R_J
196
74 R_J
83 R_J
206
188 R_J
196 R_J
210
220 R_J
224 R_J
0
4
8
12
16
20
24
RELATIVE TIME (HRS.)

Fig 10

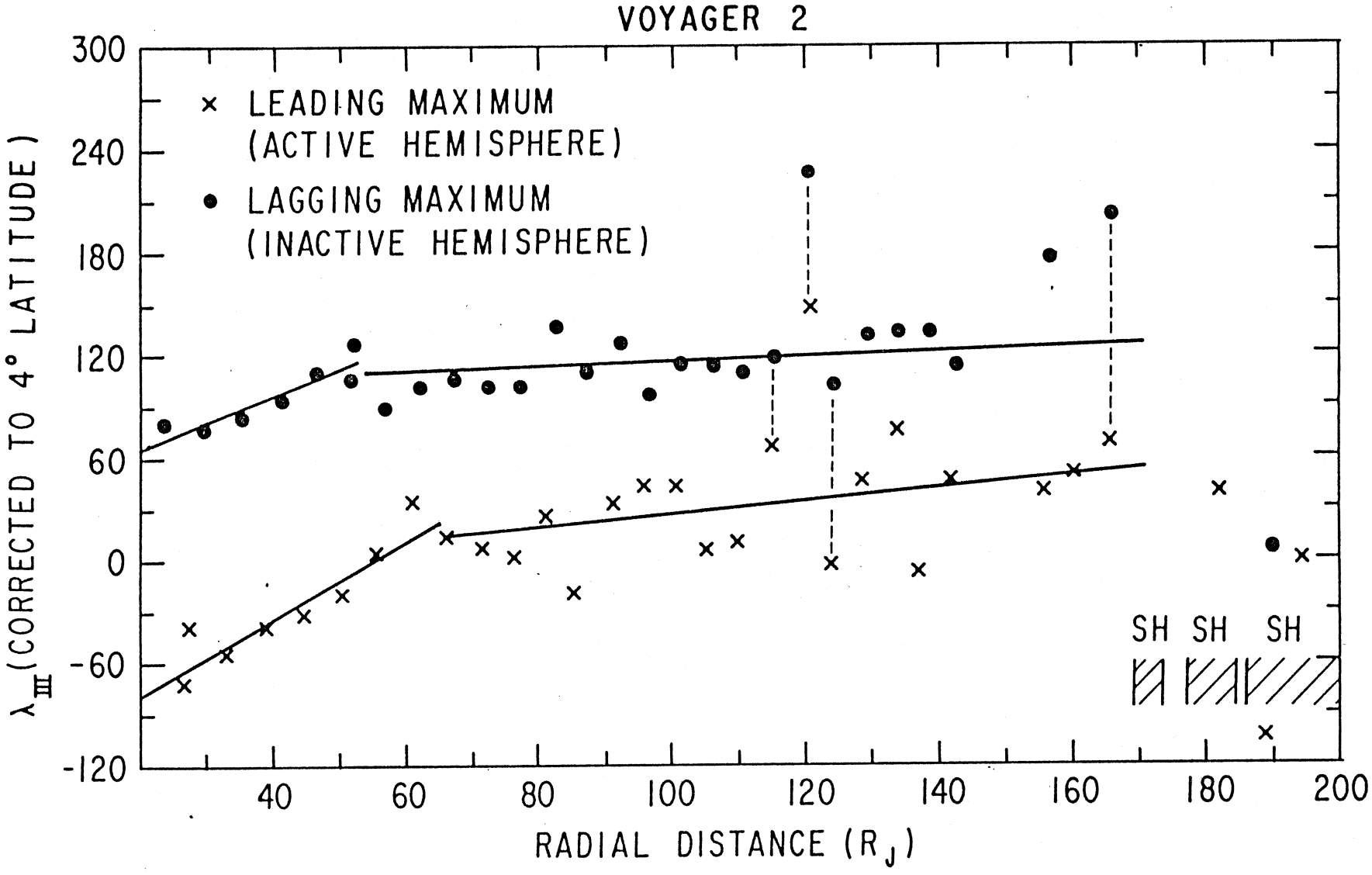
VOYAGER 2
× LEADING MAXIMUM
(ACTIVE HEMISPHERE)
• LAGGING MAXIMUM
(INACTIVE HEMISPHERE)
SH SH SH
300
240
180
120
60
0
-60
-120
40
60
80
100
120
140
160
180
200
λIII (CORRECTED TO 4° LATITUDE)
RADIAL DISTANCE (RJ)

Fig 11

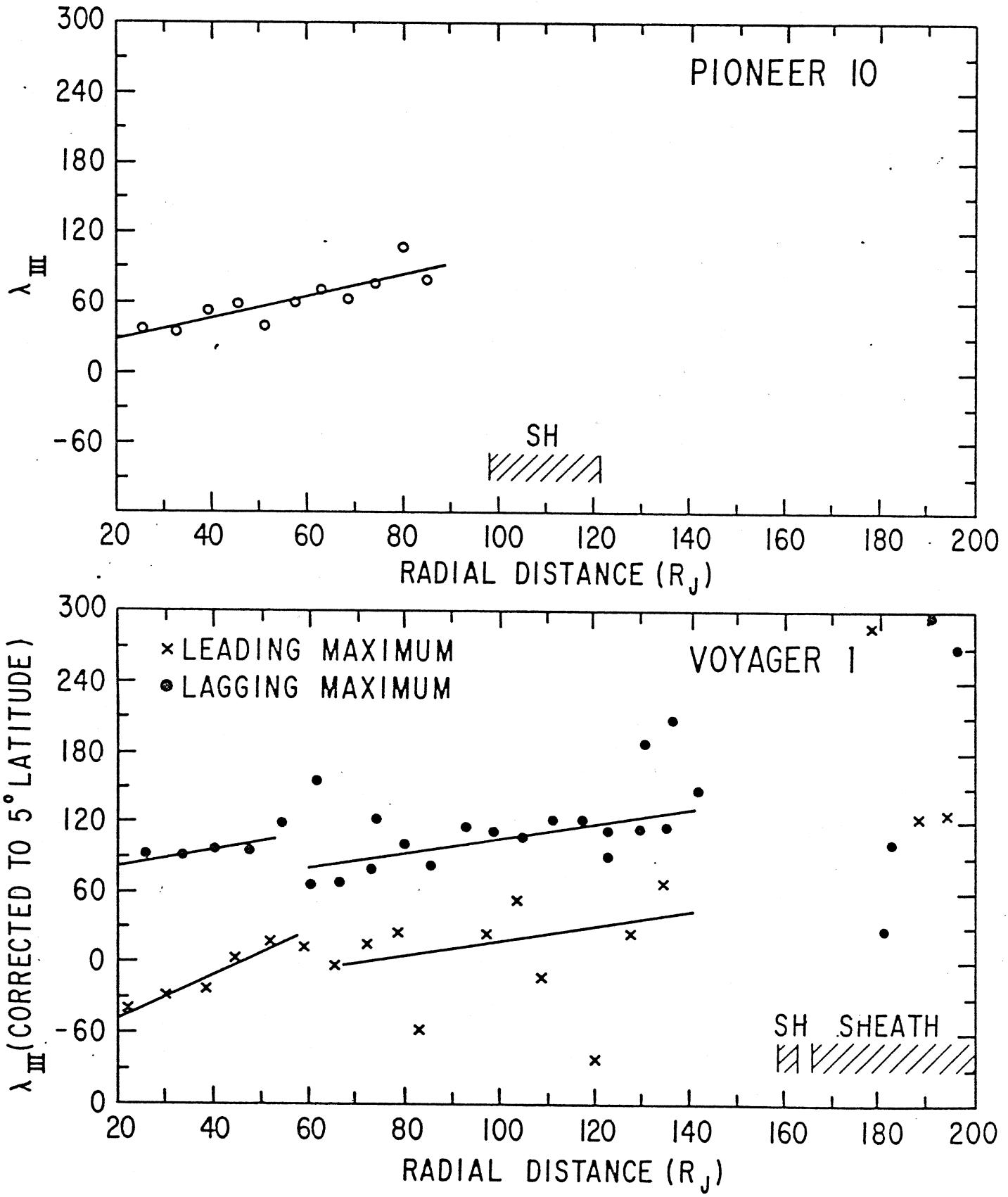
PIONEER 10
λ_{III}
300
240
180
120
60
0
-60
SH
20
40
60
80
100
120
140
160
180
200
RADIAL DISTANCE (R_J)
VOYAGER 1
× LEADING MAXIMUM
• LAGGING MAXIMUM
λ_{III} (CORRECTED TO 5° LATITUDE)
SH SHEATH
RADIAL DISTANCE (R_J)

Fig 12

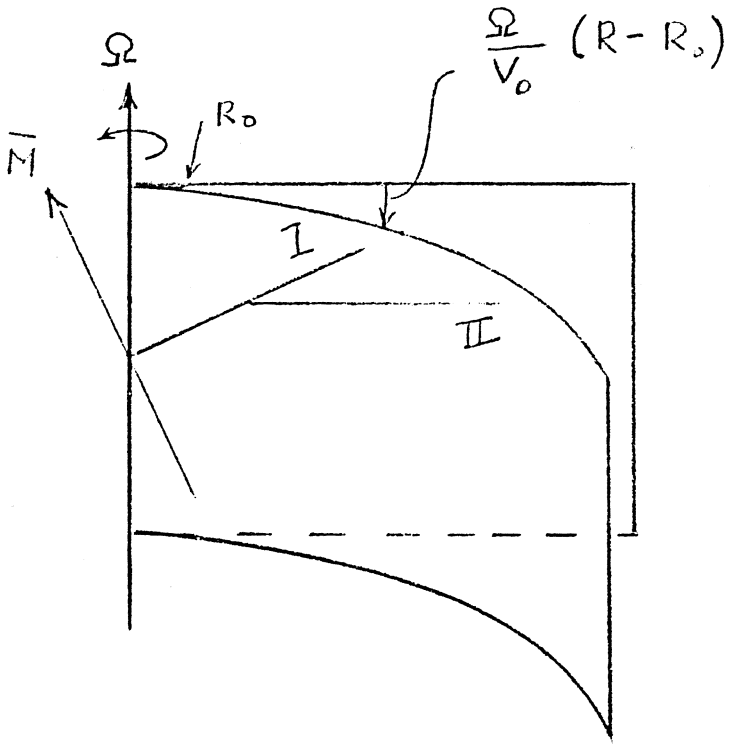

Fig 13

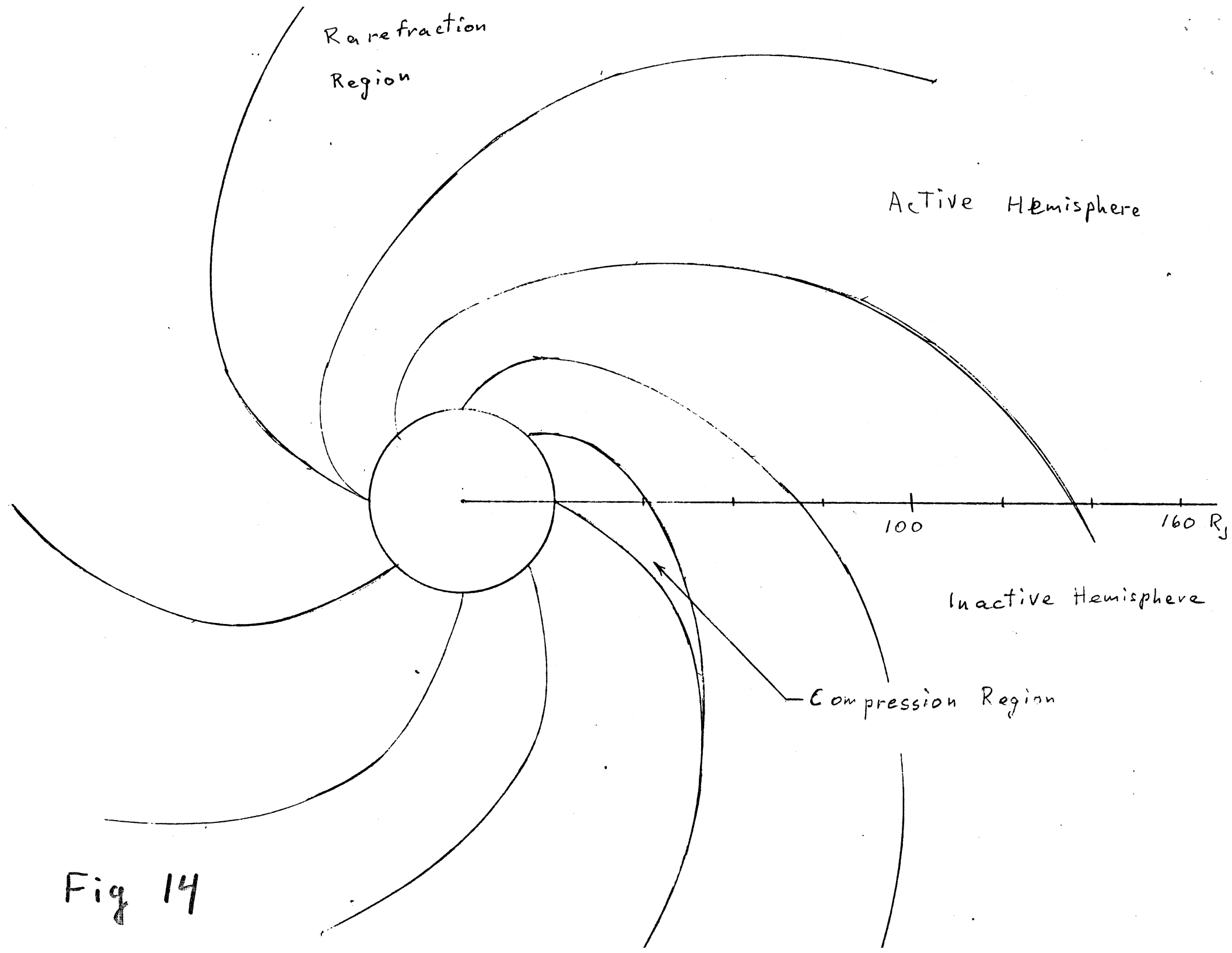
Rarefraction
Region
Active Hemisphere
100
160 R_J
Inactive Hemisphere
Compression Region

Fig 14

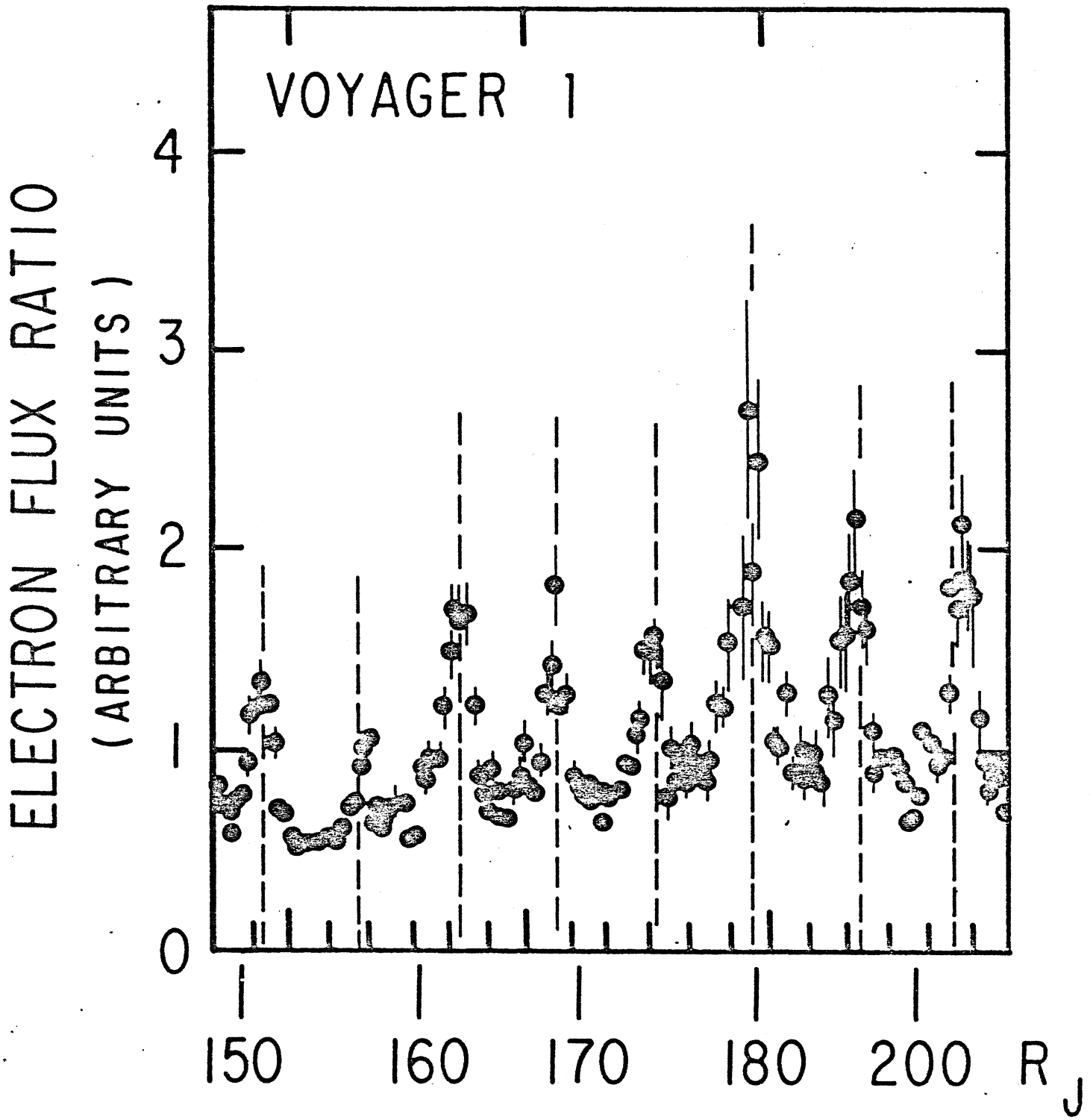
VOYAGER 1
ELECTRON FLUX RATIO
(ARBITRARY UNITS)
0
1
2
3
4
150
160
170
180
200
R J

Fig 15

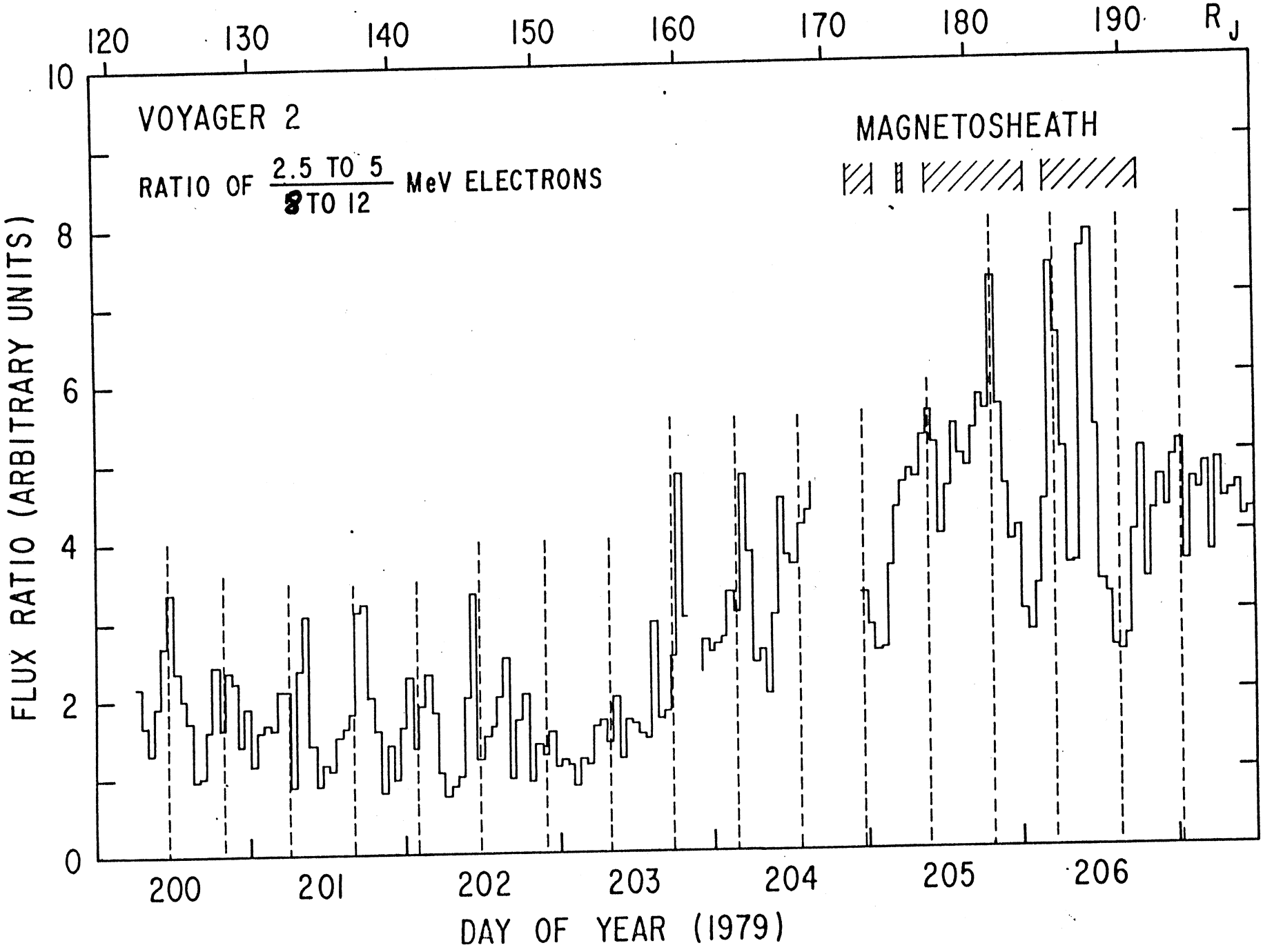
120
130
140
150
160
170
180
190
R_J
VOYAGER 2
RATIO OF 2.5 TO 5 / 8 TO 12 MeV ELECTRONS
MAGNETOSHEATH
FLUX RATIO (ARBITRARY UNITS)
0
2
4
6
8
10
200
201
202
203
204
205
206
DAY OF YEAR (1979)

Fig 16